Hydrogen and Oxygen Adsorption Stoichiometries on Silica Supported Ruthenium Nanoparticles

Romain Berthoud,[a] Pierre Délichère,[b] David Gajan,[a] Wayne Lukens,[c] Katrin Pelzer,[d] Jean-Marie Basset,[a] Jean-Pierre Candy,[a],* Christophe Copéret.[a],*

[a] Laboratoire de Chimie, Catalyse, Polymères et Procédés ESCPE Lyon 43, Bd. du 11 Novembre F-69616 Villeurbanne, France Phone : (+33) 472431811 Fax: (+33) 472431795 E-mail: coperet@cpe.fr, candy@cpe.fr

[b] Dr. P. Délichère Institut de Recherches sur la Catalyse et l'Environnement de Lyon (IRCELYON, CNRS) pierre.delichere@ircelyon.univ-lyon1.fr
Université de Lyon), 2 Avenue Albert Einstein, 69626, Villeurbanne Cedex, France.

[c] Dr. W. Lukens Chemical Sciences Division Lawrence Berkeley National Laboratory Berkeley, CA 94720, USA wwlukens@lbl.gov

[d] Dr. K. Pelzer Department for Inorganic Chemistry Fritz-Haber-Institute of the Max-Planck-Society Faradayweg 4-6, 14195 Berlin, Germany pelzer@fhi-berlin.mpg.de

ABSTRACT

Treatment under H_2 at 300 °C of Ru(COD)(COT) dispersed on silica yields 2 nm ruthenium nanoparticles, **[Ru_p/SiO_2],** according to EXAFS, HRTEM and XPS. H_2 adsorption measurements on **[Ru_p/SiO_2]** in the absence of O_2 show that Ru particles adsorb up to *ca.* 2 H per surface ruthenium atoms ($2H/Ru_s$) on various samples; this technique can therefore be used to measure the dispersion of Ru particles. In contrast, O_2 adsorption on **[Ru_p/SiO_2]** leads to a partial oxidation of the bulk at 25 °C, to RuO_2 at 200 °C and to sintering upon further reduction under H_2, showing that O_2 adsorption cannot be used to measure the dispersion of Ru particles.

KEYWORDS Ruthenium. Particles. Silica. H_2. O_2. Adsorption.

INTRODUCTION

Supported metal nanoparticles constitutes a large class of heterogeneous catalysts,[1] and their properties (activity, selectivity…) are often, if not always, associated to their size and shape.[2] Thus, a precise measurement of their size, often referred to as dispersion, is critical if one wants to understand their reactivity and try to develop structure-reactivity relationships. Of various methods targeted at measuring particles dispersion measurements, H_2 and O_2 adsorptions[3] are very useful and convenient: however this approach relies on the knowledge of the number of hydrogen adsorbed per surface atoms, and this stoichiometric ratio depends on the metals. In the case of platinum[4, 5] and rhodium,[6] extended studies on adsorption measurements, based on Langmuir adsorption isotherms, correlated to particle size distributions (determined by TEM), led to the stoichiometry of $2H/M_s$, in contrast to the former accepted value of $1H/M_s$.[7] In the case of ruthenium, early studies on Ru powders suggested a ratio of 1.5 by comparing H_2 and N_2 adsorptions.[8] Later studies on powder and supported samples[9, 10] were consistent with a stoichiometry of $1H_{irrev}/Ru_s$ (or slightly higher), which was not size dependant, while others claimed a value of $2\ H/Ru_s$.[11] It was also proposed using solid-state NMR that hydrogen chemisorption greatly underestimated the ruthenium dispersion.[12] Thus, it appears that no real consensus has been reached for the H/Ru_s stoichiometry and for the method to perform chemisorption measurements. In the case of O_2, various studies on ruthenium diverged in the O/Ru_s stoichiometry, ranging from 1 to 2,[10, 13] but agreed on its high dependence toward the method of preparation and the size of the particles.

Here, by using EXAFS, HRTEM and XPS in combination with H_2 adsorption measurements, we show that fully reduced Ru_P supported on silica, **$[Ru_P/SiO_2]$,** (reproducibly and reversibly) adsorb $2H/Ru_s$. We also show that adsorption of O_2 leads to partial oxidation of the bulk at 25 °C. Finally, while oxidation/reduction cycles do not significantly affect the O adsorption on Ru_t, we show that the H_2 adsorption varies, which is consistent with a sintering of the particles after each cycle.

EXPERIMENTAL

1. Materials

All experiments were carried out under dry and oxygen free Ar using either standard Schlenk or glove-box techniques for organometallic synthesis. For the syntheses and the treatments of the surface species, reactions were carried out using high vacuum lines (10^{-5} mbar) and glove-box techniques. H_2 (reactants and adsorbates) was purified over R3-11 BASF catalyst / MS 4 Å prior to use. O_2 was dried over MS 4 Å prior to use. Pentane was distilled from NaK under N_2. Elemental analyses were performed at the CNRS Central Analysis Department of Solaize (Ru) and at the University of Bourgogne, Dijon (C H).

Two types of catalysts were prepared for adsorption measurements, namely **[Ru_p/SiO_2]** and **[Ru_p/SBA-15]**. Silica (Aerosil Degussa, 200 m^2g^{-1}) was compacted with distilled water, calcined at 500 °C under air for 2 h and treated under vacuum (10^{-5} mbar) at 500 °C for 12 h and then at 700 °C for 4 h (support referred to as $SiO_{2\text{-}(700)}$). SBA-15 was prepared from $Si(OEt)_4$ according to literature conditions,[14] calcined at 500 °C under air for 5 h and then treated under vacuum at 500 °C for 15 h (support referred as SBA-$15_{(500)}$). The supported Ru particles were prepared by adapting a literature procedure [15] as follows: typically, Ru(COD)(COT)[16] and $SiO_{2\text{-}(700)}$ (or SBA-$15_{(500)}$) were loaded in a 370-mL reactor, and *ca.* 3 mL of pentane were added. This mixture was stirred to insure a homogeneous dispersion of the complex on the support. The solvent was evaporated to dryness, and this procedure was repeated twice. The solid was finally dried under vacuum (10^{-5} mbar) for 1 h, yielding a yellow powder. Then, this solid was loaded in a 470 mL reactor flask at 25 °C, H_2 (666 mbar) was added, and the reactor was heated at 300 °C for 24 h. After evacuation of the gas phase at 25 °C, a second H_2 treatment under the same reaction conditions was performed. Finally, the reactor is evacuated under vacuum (10^{-5} mbar) for 30 min, yielding Ru_p/SiO_2, 0.65 $\%_{wt}$ Ru (or Ru_p/SBA-15, 1.92 $\%_{wt}$ Ru). For all the samples prepared, no carbon is detected by elemental analysis (< 0.1 $\%_{wt}$).

2. XPS

X-ray photoelectron spectroscopy was performed in a KRATOS Axis Ultra DLD spectrometer, using a monochromated Al Kα x-ray with a pass energy of 20 eV and a coaxial charge neutraliser. The base pressure in the analysis chamber was better than 5 10^{-8} Pa. The samples were prepared in a glove-box on an Indium foil sample holder and transferred into the spectrometer under inert atmosphere.

XPS spectra of Ru3d, C1s, Si2p and O1s levels were measured at a normal angle with respect to the plane of the surface. High-resolution spectra were corrected for charging effects by assigning a value of 284.6 eV to the C1s peak (adventitious carbon). Binding energies were determined with an accuracy of ± 0.2 eV. Synthetic components on Ru3d-C1s were analysed with a Shirley background subtraction and a peak shape with a combination of Gaussian and Lorentzian (30% Lorentzian).

3. Determination of particle size by TEM

All samples for TEM analysis were prepared from powder samples by dry preparation in a glove box and *were transferred inside a special vacuum transfer holder under inert atmosphere* to a Philips CM200 Transmission Electron Microscope. The acceleration voltage was 200 kV.

4. Determination of particle size by EXAFS

Transmission data were obtained at Stanford Synchrotron Radiation Laboratory on beam-line 11-2. The data reduction was performed by standard procedures using the programs EXAFSPAK and Athena.[17][18] The background was removed by fitting a polynomial to the pre-edge of the data such that the post-edge spectrum followed the

Victoreen function μ_{Vic}. The reduced sample was loaded in the glove-box in a cell tightly closed with aluminized mylar windows.

Fitting of the spectrum was done on the k^3 weighted data using Artemis/ifeffit.[18, 19] The program FEFF7 was used to calculate theoretical values for S_i, F_i, λ_i, ϕ_i, and ϕ_c.[20] The ΔE_0 parameter was allowed to vary during fitting of the EXAFS spectra; for a given fit, ΔE_0 was constrained to be the same for all scattering shells. ΔE_0 is referenced to the inflection point of the absorption edge. The value of S_0^2 was determined to be 0.66 by fitting the EXAFS spectrum of bulk Ru. The fit ranges are given by Δk and ΔR. Δk is the range in k-space over which the spectrum can be fit and is determined by the quality of the data. ΔR is the range in R-space over which the data is being fit ; R_{max} and R_{min} are chosen at the points where the spectrum has a minimum at the end and beginning of the range of data being fit. The number of independent points, N_{ind}, is given by Stern rule, $N_{ind} = 2+2\Delta k \Delta R/\pi$.[21]

5. Adsorption experiments

Adsorption of H_2. Chemisorption experiments were carried out at 25 °C using conventional Pyrex volumetric adsorption equipment.[22] The vacuum (10^{-6} mbar) was achieved with a liquid nitrogen-trapped mercury diffusion pump. The equilibrium pressure was measured with a Texas Instrument gauge (pressure range, 0–1000 mbar with an accuracy of 0.1 mbar). The catalyst sample was placed in a Pyrex cell and out-gassed at 25 °C before applying a thermal treatment under vacuum at 300 °C for 3 h (ramp of 3 °C/min up to 300 °C), and then the chemisorption measurements were performed at 25 °C. Reversible adsorption values are measured after out-gassing the samples at 25 °C for 3 h. The oxidation/reduction cycles were performed in a reactor designed to avoid contact of the sample with the atmosphere. Typically, the sample was reduced under a H_2 flow at 300 °C during 3 h, followed by a desorption at 300 °C for 3 h and an adsorption of H_2 at 25 °C. The H/Ru ratios are measured at 25 °C under [0-250] mbar of H_2.

Adsorption of O_2. After desorption at 300 °C for 3 h of silica supported particles, previously obtained by reaction under H_2 at 300 °C, adsorption of O_2 was performed at 25 °C and higher temperatures, and the O/Ru ratios are measured at 25 °C under [0-250] mbar of O_2.

RESULTS AND DISCUSSION

1. Characterisation of ***[Ru_p/SiO_2]*** *by XPS*

The XPS spectrum of Ru_p/SiO_2 (sample **1**) at the Ru 3d level shows a binding energy of the Ru $3d_{5/2}$ at 280.2 eV (Fig. 1), which is consistent with $Ru^{(0)}$[23] [24] of a totally reduced ruthenium sample, a crucial point for H_2 adsorption measurements.

2. Determination of the dispersion by Transmission Electron Microscopy

The TEM images of **[Ru_P/SiO_2]** (sample **2**), *never exposed to air or O_2*, show homogeneously dispersed particles (Fig. 2a) with a narrow particle size distribution centred at 2.0 ± 0.3 nm (Fig. 2b). This is observed reproducibly with other **[Ru_P/SiO_2]** samples. Assuming that these particles adopt a hcp structure as for bulk Ru and small nanoparticles,[25] the dispersion can be estimated to *ca.* 55 % (Fig. 2c). Note that, when the samples are exposed to air (before introduction in the microscope as typically done in TEM analysis), the particles are difficult to observe. This is probably due to the formation of a RuO_2 shell around the particles, which induces a loss of contrast. This could also explain the discrepancies between various reported data (vide supra).

3. Calculation of the dispersion by EXAFS

The EXAFS spectrum of a **[Ru_P/SiO_2]** sample (Ru 0.9 $\%_{wt}$), its Fourier transform, and their corresponding fits are shown in Fig. 3. Fitting the EXAFS data, using a model for Ru nanoparticles, gives a contribution of 10 neighbours in the first 2 shells (1.64-1.67 Å) (Table 1), which is consistent with nanoparticles having a mean size of 2.3 ± 0.7 nm.[26] This result is fully consistent with what is observed by HR-TEM.

4. Hydrogen and oxygen adsorption

First, the adsorption isotherms of H_2 (total and reversible) can be calculated assuming a dissociative adsorption on the surface ruthenium atoms, following the Langmuir law, as described in eq. 1, where Q_{irr} and Q_{rev} are respectively the amount of hydrogen irreversibly and reversibly adsorbed at room temperature, k is the reversible adsorption constant and P is the hydrogen pressure, note that Q_{irr} is not sensitive to P.[27]

$$Q_{ads}=Q_{irr}+Q_{rev}.(kP)^{1/2}/[1+(kP)^{1/2}] \qquad (1)$$

The experimental and calculated values obtained for **[Ru_P/SiO_2]** are reported on Fig. 4 **(sample 2**) and Table 2. The values of H/Ru_t correspond to extrapolation to infinite equilibrium pressure. Note that no measurable adsorption occurs on the support alone, and that adsorption of H_2 on **[Ru_P/SiO_2]** reaches rapidly a plateau; these data are consistent with the absence of spill-over on the support. The silica supported ruthenium particles **[Ru_P/SiO_2]** adsorb 1.09 H/Ru_t at equilibrium (Sample **2**, Table 2). Considering a dispersion of 55 % (TEM), the stoichiometry is therefore 2.0 H/Ru_s. In the case of isotherms of reversible H_2, the amount of H adsorbed on Ru is 0.70 H/Ru_t. which corresponds to 2/3 of the total amount. These H species correspond to more weakly adsorbed hydrogen on the surface, which are easily removed by evacuating the sample under vacuum at 25 °C. Note that the value of $2H/Ru_s$ is obtained reproducibly on a wide range of samples prepared at different loadings (0.66-1.92 $\%_{wt}$) using non-porous ([**Ru_P/SiO_2**] – Samples 1-3) or mesoporous silica (**[Ru_P/SBA-15]**).

Second, adsorptions of O_2 have been performed (Table 3). At 25 °C, 1.4-1.5 O/Ru_t were adsorbed irreversibly, and these values increased with time and temperature to reach the stable values of 1.9 O/Ru_t after treatment at 200 °C for 2 h, which is in agreement with the formation of bulk RuO_2.

Finally, the influence of oxidation/reduction cycles on H_2 and O_2 adsorptions has been studied (sample **2** of **[Ru_p/SiO_2]**, Table 4). Although the H/Ru_t ratio decreases from 1.07 to 0.73 after the first oxidation/reduction cycle, the O/Ru_t ratio (25 °C) remains almost constant (from 1.39 to 1.52). As further oxidation/reduction cycles are performed on this sample, the H/Ru_t ratio slowly decreases while the O/Ru_t ratio remains constant. This phenomenon is consistent with a modification of the particles, probably sintering, upon oxidation/reduction cycles.

CONCLUSION

In conclusion, elemental analysis, XPS, EXAFS, TEM and adsorption measurements on **[Ru_p/SiO_2]** show that:

(1) Fully reduced 2 nm size Ru nanoparticles supported on silica, free of strong ligands, such as CO or Cl^-, and carboneous species, are obtained using a perhydrocarbyl complex as precursor.

(2) Ru particles adsorbs *ca.* 2 H per surface ruthenium atoms ($2H/Ru_s$) on various samples, so that this technique can be used to measure the dispersion of Ru particles.

(3) O_2 is an inappropriate probe for dispersion measurements because of partial oxidation of the bulk even at 25 °C and the modification of adsorption properties upon oxidation/reduction cycles.

Finally, it is also worth pointing out that the H/M stoichiometry ($2\ H/Ru_s$) is very close to this already obtained for Pt and Rh particles,[4, 6] and we are currently investigating the generality of this observation on other metal particles.

AKNOWLEDGMENTS

RB and DG thank le Ministère de la Recherche et de l'Education and the Région Rhône-Alpes (Cluster 5) for graduate fellowships, respectively. We are all grateful to the CNRS (PICS program), CPE Lyon and IDECAT for financial supports. Portions of this work were performed at the LBNL, supported by the Director, Office of Science, Office of Basic Energy Sciences of the US Department of Energy under contract No. DE-AC02-05CH11231, and at the Stanford Synchrotron Radiation Laboratory, a national user facility operated by Stanford University on behalf of the U.S. Department of Energy, Office of Basic Energy Sciences.

REFERENCES

[1] T. Bell Alexis, *Science* **2003**, *299*, 1688-1691.

[2] M. Comotti, C. Della Pina, R. Matarrese, M. Rossi, *Angew. Chem. Int. Ed.* **2004**, *43*, 5812-5815; M. Frank, M. Baumer, *Phys. Chem. Chem. Phys* **2000**, *2*, 3723-3737; C. R. Henry, *Appl. Surf. Sci.* **2000**, *164*, 252-259.

[3] G. K. Boreskov, A. P. Karnaukhov, *Zhur. Fiz. Khim.* **1952**, *26*, 1814-1823; L. Spenadel, M. Boudart, *J. Phys. Chem.* **1960**, *64*, 204-207.

[4] J. P. Candy, P. Fouilloux, A. J. Renouprez, *J. Chem.Soc., Faraday I* **1980**, *76*, 616-629.

[5] C. Hubert, A. Frennet, *Catal. Today* **1993**, *17*, 469-482.

[6] J. P. Candy, A. El Mansour, O. A. Ferretti, G. Mabilon, J. P. Bournonville, J. M. Basset, G. Martino, *J. Catal.* **1988**, *112*, 201-209.

[7] H. Calvin, H. Bartholomew, *Roy. Soc. Chem.* **1994**, *11*, 93-126.

[8] H. Kubicka, *J. Catal.* **1968**, *12*, 223-237.

[9] R. A. Dalla Betta, *J. Catal.* **1974**, *34*, 57-60; R. A. Dalla Betta, *J. Phys. Chem.* **1975**, *79*, 2519-2525; R. A. Dalla Betta, M. Shelef, *J. Catal.* **1977**, *48*, 111-119; H. Y. Lin, Y. W. Chen, *Thermochim. Acta* **2004**, *419*, 283-290; J. Garcia-Anton, R. Axet, S. Jansat, K. Philippot, B. Chaudret, T. Pery, G. Buntkowsky, H.-H. Limbach, *Angew. Chem. Int. Ed.* **2008**, *47*, 1-6.

[10] J. G. Goodwin, Jr., *J. Catal.* **1981**, *68*, 227-232.

[11] G. Lauth, E. Schwarz, K. Christmann, *J. Chem. Phys.* **1989**, *91*, 3729-3744.

[12] S. Y. Chin, O. S. Alexeev, D. Amiridis, *Appl. Catal A: General* **2005**, *286*, 157-166.

[13] N. E. Buyanova, A. P. Karnaukhov, N. G. Koroleva, I. D. Ratner, O. N. Chernyavskaya, *Kinet. Katal.* **1972**, *13*, 1533-1539; K. C. Taylor, *J. Catal.* **1975**, *38*, 299-306; H. Kubicka, *React. Kinet. Catal. L.* **1976**, *5*, 223-228; H. Kubicka, B. Kuznicka, *React. Kinet. Catal. L.* **1978**, *8*, 131-136; G. Corro, R. Gomez, *React. Kinet. Catal. L.* **1979**, *12*, 145-150; P. G. J. Koopman, A. P. G. Kieboom, H. Van Bekkum, *J. Catal.* **1981**, *69*, 172-179.

[14] D. Zhao, Q. Huo, J. Feng, B. F. Chmelka, G. D. Stucky, *J. Am. Chem. Soc.* **1998**, *120*, 6024-6036.

[15] N. Kitajima, A. Kono, W. Ueda, Y. Morooka, T. Ikawa, *J. Chem. Soc. Chem., Commun.* **1986**, 674-675.

[16] P. Pertici, G. Vitulli, *Inorg. Synth.* **1983**, *22*, 176-181.

[17] Koningsberger, D. C.; Prins, R. X-Ray Absorption: Principles, Applications, Techniques of EXAFS, SEXAFS, and XANES; John Wiley & Sons: New York, 1988.

[18] B. Ravel, M. Newville, *Phys. Scripta* **2005**, *T115*, 1007-1010.

[19] M. Newville, *J. Synchrotron Rad.* **2001**, *8*, 322-324.

[20] J. J. Rehr, R. C. Albers, S. I. Zabinsky, *Phys. Rev. Lett.* **1992**, *69*, 3397-3400.

[21] E. A. Stern, *Phys. Rev. B* **1993**, *48*, 9825-9827.

[22] J. P. Candy, A. E. Mansour, O. A. Ferretti, G. Mabilon, J. P. Bournonville, J. M. Basset, G. Martino, *J. Catal.* **1988**, *112*, 201-209.

[23] N. Chakroune, G. Viau, S. Ammar, L. Poul, D. Veautier, M. M. Chehimi, C. Mangeney, F. Villain, F. Fievet, *Langmuir* **2005**, *21*, 6788-6796; V. Mazzieri, F. Coloma-Pascual, A. Arcoya, P. C. L'Argentiere, N. S. Figoli, in *Appl. Surf. Sci., Vol. 210*, **2003**, pp. 222-230; K. W. Park, J.-H. Choi, B.-K. Kwon, S.-A. Lee, Y.-E. Sung, H.-Y. Ha, S.-A. Hong, H. Kim, A. Wieckoski, *J. Phys. Chem. B* **2002**, *106*, 1869; C. D. Wagner, W. M.

Riggs, L. E. Davis, F. J. Moulder, G. E. Muilenberg, in *Physical Electronics Division, Perkin-Elmer, Vol. 55*, Eden Prairie, MN, **1979**, p. 344.

[24] Note that the binding energies of Si 2p and O 1s are found at 103.6 and 532.9 eV respectively which are the exact values expected.

[25] K. Pelzer, O. Vidoni, K. Philippot, B. Chaudret, V. Collière, *Adv. Funct. Mater.* **2003**, *13*, 118-126; K. Pelzer, B. Laleu, F. Lefebvre, K. Philippot, B. Chaudret, J. P. Candy, J. M. Basset, *Chem. Mat.* **2004**, *16*, 4937-4941; D. Wostek-Wojciechowska, J. K. Jeszka, C. Amiens, B. Chaudret, P. Lecante, *J. Colloid Interf. Sci.* **2005**, *287*, 107-113.

[26] S. Calvin, S. X. Luo, C. Caragianis-Broadbridge, J. K. McGuinness, E. Anderson, A. Lehman, K. H. Wee, S. A. Morrison, L. K. Kurihara, *Appl. Phys. Lett.* **2005**, *87*, 233102/233101-233102/233103.

[27] The full adsorption models should be defined as $Q_{ads}=Q_{irr}.(k_{irr}P)^{1/2}/[1+(k_{irr}P)^{1/2}]+Q_{rev}.(k_{rev}P)^{1/2}/[1+(k_{rev}P)^{1/2}]$, but it simplifies to $Q_{ads}=Q_{irr}+Q_{rev}.(kP)^{1/2}/[1+(kP)^{1/2}]$, because $Q_{irr}\approx(Q_{irr}.(k_{irr}P)^{1/2}/[1+(k_{irr}P)^{1/2}]$ as the values obtained for $k_{irr}P$ are always >> 1.

Table 1. Fitted EXAFS parameters for **[Ru_p/SiO_2]**[a].

Neighbor	Number of Neighbors[b]	Distance (Å)	σ^2 (Å^2)
Ru	4.9(3)	2.634(2)	0.0058(2)
Ru	4.9(3)	2.679(2)[c]	0.0058[c]
Ru	4.5(4)	3.76(1)	0.008(1)
Ru	1.4(2)	4.4(1)	0.013(2)
Ru	12(2)	4.64(2)	0.0130[d]
Ru	8(1)	5.06(7)	0.0130[d]
Ru[e]	3.9(6)	5.30(3)	0.0130[d]

Fit range: 2 Å^{-1} < k < 15 Å^{-1}; 1.63 Å < R < 5.87 Å

# of independent points: 37

# of parameters: 11

R_factor: 0.014

a) S_0^2=0.66 (fixed, determined from fitting Ru foil), ΔE_0 = -8(1) eV, R = 11(3) Å

b) # of neighbors, N, determined using the formula for nanoparticles: $N=N_0[1-(3/4)(r/R)+(1/16)(r/R)^3]$, where N_0 is the coordination number for that shell in Ru metal (hcp structure), R is the radius of the particles, and r is the Ru-Ru distance of that set of atoms.[26]

c) The hcp structure of Ru contains two sets of 6 atoms, which have slightly different bond distances. Only change in bond distance and the Debye-Waller factor was used in fitting the first two shells.

d) Debye-Waller factor same as for the fourth shell of atoms at 4.4 Å.Shell includes contributions from two multiple-scattering paths, which have the same parameters as the single scattering path.

e) Shell includes contributions from two multiple-scattering paths, which have the same parameters as the single scattering path.

Table 2. H_2 adsorption on **[Ru_p/SiO_2]**.

Sample	Ru /%$_{wt}$	Q_{irr} (Q_{rev}) /mMol.g^{-1}	k /mbar^{-1}	H/Ru_t
[Ru_p/SiO_2] Sample 1	0.66	0.0145 (0.017)	0.18	0.96
[Ru_p/SiO_2] Sample 2	0.83	0.010 (0.029)	0.18	1.09
[Ru_p/SBA-15]	1.92	0.032 (0.072)	0.50	1.09

Table 3. O_2 adsorption on **[Ru_p/SiO_2]**.

Sample	Experimental value	
	O/Ru_t (25 °C)	O/Ru_t (200 °C)
[Ru_p/SiO_2] Sample 2	1.40	-
[Ru_p/SiO_2] Sample 3	1.44	1.87

Table 4. H_2 and O_2 adsorption on **[Ru_p/SiO_2]** as a function of the number of oxidation/reduction cycles.

Cycle	Experimental values	
	H_t/Ru	O/Ru (25 °C)
0	1.07	1.39
1	0.73	1.52
2	0.68	1.46
3	0.58	-

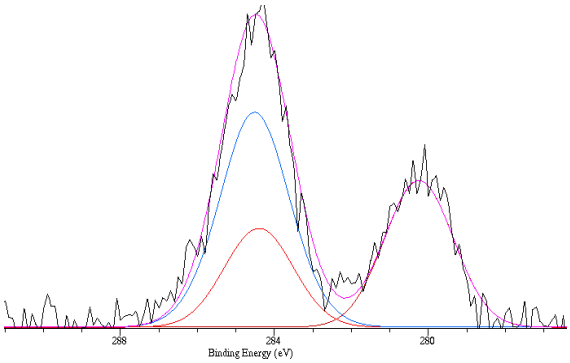

Figure 1. XPS spectrum of **[Ru_p/SiO_2]** (purple) at the Ru 3d level with the Ru 3d (red) and C 1s (blue) contributions.

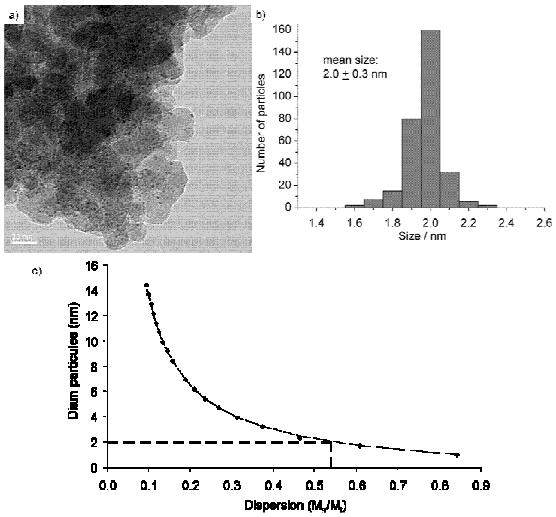

Figure 2. Transmission Electron Microscopy of **[Ru_p/SiO_2]** (sample **2**, 0.83 $\%_{wt}$ Ru).a) TEM image at a 20 nm scale. b) Particle size distribution. c) Determination of the dispersion using idealized hcp structure of ruthenium particles.

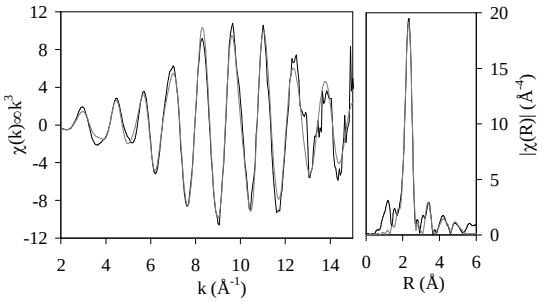

Figure 3. EXAFS spectrum and Fourier Transform of **[Ru_p/SiO_2]**. Data is black and fit is grey.

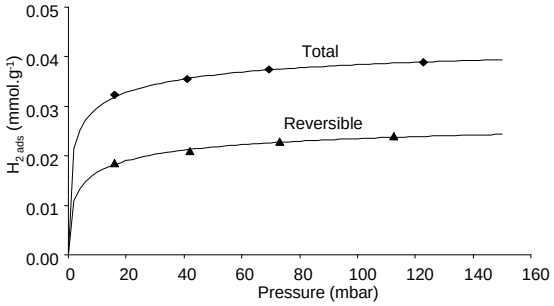

Figure 4. Hydrogen adsorption on **[Ru_p/SiO_2]** (sample 2). ◆ Total adsorption. ▲ Reversible adsorption. ▬ Simulated Langmuir adsorption isotherms.

Table 5. Fitted EXAFS parameters for **[Ru_p/SiO_2]**[a].

Table 6. H_2 adsorption on **[Ru_p/SiO_2]**.

Table 7. O_2 adsorption on **[Ru_p/SiO_2]**.

Table 8. H_2 and O_2 adsorption on **[Ru_p/SiO_2]** as a function of the number of oxidation/reduction cycles.

Figure 1. XPS spectrum of **[Ru_p/SiO_2]** (purple) at the Ru 3d level with the Ru 3d (red) and C 1s (blue) contributions.

Figure 2. Transmission Electron Microscopy of **[Ru_p/SiO_2]** (sample **2**, 0.83 $\%_{wt}$ Ru).a) TEM image at a 20 nm scale. b) Particle size distribution. c) Determination of the dispersion using idealized hcp structure of ruthenium particles.

Figure 3. EXAFS spectrum and Fourier Transform of **[Ru_p/SiO_2]**. Data is black and fit is grey.

Figure 4. Hydrogen adsorption on **[Ru_p/SiO_2]** (sample 2). ◆ Total adsorption. ▲ Reversible adsorption. ▬ Simulated Langmuir adsorption isotherms.